Razi University

Journal of
Applied Research in Water & Wastewater

Journal homepage: www.arww.razi.ac.ir

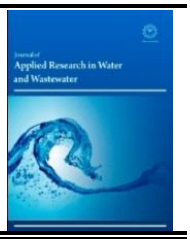

Original paper

Removal, preconcentration and determination of methyl red in water samples using silica coated magnetic nanoparticles

Masoud Shariati-Rad[1]*, Mohsen Irandoust[1], Somayyeh Amri[1], Mostafa Feyzi[2], Fattaneh Ja'fari[2]

[1]*Department of Analytical Chemistry, Faculty of Chemistry, Razi University, Kermanshah 6714967346, Iran.*
[2]*Department of Physical Chemistry, Faculty of Chemistry, Razi University, Kermanshah 6714967346, Iran.*

ARTICLE INFO

Article history:
Received 18 August 2013
Received in revised form 19 November2013
Accepted 14 March 2014
Available online 28 March 2014

Keywords:
Methyl red
Magnetic nanoparticles
Central composite design
Removal
Preconcentration

ABSTRACT

A method was developed for removal, preconcentration and spectrophotometric determination of trace amounts of methyl red based on SiO_2-coated Fe_3O_4magnetic nanoparticles. The influence of pH, dosage of adsorbent and contact time on the adsorption of dye was explored by central composite design. The kinetic data were analyzed based on the Langmuir and Freundlich adsorption isotherms. The Langmuir model was fitted well to data and the maximum monolayer capacity q max of 49.50 mg g^{-1} was calculated. The results showed that desorption efficiencies of higher than 99% can be achieved in a short contact time of 3 min and in one step elution using 2.0 mL of 0.1 mol L^{-1} NaOH. The magnetic nanoparticles were washed with deionized water and reused for two successive removal processes with removal efficiencies more than 90%. Then desorbed dye was determined spectrophotometrically. The calibration curve was linear in the range of 0.025–0.250 mg L^{-1} of dye with a correlation coefficient of 0.9922. The relative standard deviations obtained upon application of the method to the real samples were lower than 0.7%. A preconcentration factor of the method was 50.

© 2014 Razi University-All rights reserved.

1. Introduction

Dye removal from wastes has been the object of many researches in the past few years because of the potential toxicity of dyes and visibility problems (Afkhami et al. 2010). These compounds are used in large quantity in many industries including textile, leather, cosmetics, paper, printing, plastic, pharmaceutical and food to color their products (Shariati et al. 2011). As a result, considerable amounts of colored wastewater are generated (Afkhami and Moosavi 2010). Many of the industrial dyes are toxic, carcinogenic, mutagenic and teratogenic. Their removal from wastewater is of great interest (Qadri et al. 2009).

The methods used to remove organic dyes and pigments from wastewaters are classified into three main categories: (i) physical (adsorption, filtration, and flotation) (Afkhami and Moosavi 2010; Qadri et al. 2009; Kannan and Sundaram 2001; Wang et al. 2006), (ii) chemical (oxidation, reduction, and electrochemical) (Arslan and Balcioglu 2001; Tsui and Chu 2001; Gutierrez et al. 2002) and (iii) biological (aerobic and anaerobic degradation) (Stolz 2001; Bell and Buckley 2003; Haghighi-Podeh et al. 2001; Kapdan and Ozturk 2005). Two most available technologies for dye removal are oxidation and adsorption. Oxidation methods are probably the best technologies to eliminate organic carbons completely but they are only effective for wastewaters with very low concentrations of organic compounds (Sun and Xu 1997).

Adsorption has been found to be superior to the other techniques for removal of colors, odor, oils and organic pollutants from process or waste effluent treatments in terms of initial cost, simplicity of design and ease of operation (Juang et al. 2002). Because of its capability for efficient adsorbing of a broad range of compounds, the most efficient adsorbing of a broad range of compounds, the most commonly used adsorbent for color removal is activated carbon (Afkhami et al. 2010). The main disadvantage of the activated carbon is its high production and treatment costs (Afkhami et al. 2010).

Recently, numerous approaches have been studied for the development of alternative effective adsorbents. Some of the reported sorbents include clay materials, zeolites, siliceous material, agricultural wastes, industrial waste products and biosorbents such as chitosan and peat (Mirsha and Bajpaj 2006; Aleboyeh and Aleboyeh 2006).

Magnetic nanoparticles (MNPs) have been recognized as efficient adsorbents with large specific surface area and small diffusion resistance. Moreover, the magnetic separation provides suitable route for online separation (Qadri et al. 2009).

Iron oxide MNPs are superparamagnetic. This means that when they have been adhered to the target compounds, they can quickly be removed along with them from a matrix using a magnetic field.

In the past decade, the synthesis of spinel magnetite and maghemite nanoparticles has been intensively developed not only for their great fundamental scientific interest but also for many technological applications. These applications include in biology such as extraction of genomic DNA (Xie et al. 2004), contrast agents in magnetic resonance imaging (MRI) (Bulte 2006), medical applications (such as targeted drug delivery) (Laurent et al. 2008), bioseparation (Bucak et al. 2003), separation and preconcentration of various anions and cations (White et al. 2009; Zhou et al. 2009; Tuutijarvi et al. 2009). Silica has been considered as one of the most ideal shell materials due to its chemical stability and versatility in surface modification via Si–OH groups (Santhi et al. 2010).

Corresponding author E-mail: mshariati_rad@yahoo.com

Please cite this article as: M. Shariati-Rad, M. Irandoust, S. Amri, M. Feyzi, F. Ja'fari, Removal, preconcentration and determination of methyl red in water samples using silica coated magnetic nanoparticles and central composite design, Journal of Applied Research in Water and Wastewater, 1(1), 2014, 6-12.

Application of experimental design in decolorization processes has been reported. It has been proven that it is a powerful tool for the optimization of degradation (Torrades and Garcia-Montano, 2014; Sahoo and Gupta 2012; Zuorro et al. 2013) or adsorption (de Sales et al. 2013; Ravikumar et al. 2006; Singh et al. 2011; Gomez and Pilar Callao 2008) of different dyes.

In this study, SiO_2-coated Fe_3O_4 magnetic nanoparticles were synthesized and employed for removal, preconcentration and determination of methyl red in water samples using experimental design and spectrophotometry. It is the first report on the application of SiO_2-coated Fe_3O_4 magnetic nanoparticles and experimental design for preconcentration, determination and removal of methyl red in environmental water samples. The kinetics of adsorption of methyl red onto the SiO_2-coated Fe_3O_4 magnetic nanoparticles was investigated. Additionally, the recovery of the dye from the nanoparticles using different solvents is described.

2. Experimental

2.1. Reagents and materials

All the chemicals and reagents used in this work were of analytical grade. Iron nitrate $Fe(NO_3)_3.9H_2O$ (99%), tetra ethoxysilane (TEOS) (98%) and oxalic acid $H_2C_2O_4.2H_2O$ were purchased from Merck (Darmstadt, Germany). Structural formula of methyl red has been shown in Scheme 1. Double distilled water was used throughout the study. The stock 500 mgL^{-1} solution of methyl red was prepared in double distilled water and experimental solutions of the desired concentrations were obtained by successive dilutions of the stock solution with double distilled water. The initial pH was adjusted with 0.1 mol L^{-1} solutions of HCl or NaOH. All the adsorption experiments were carried out at room temperature.

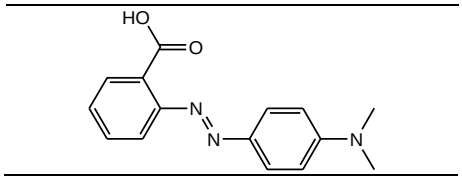

Scheme 1. Molecular structure of methyl red.

2.2. Instrumentation

An Agilent model 8453 spectrophotometer with diode array detector was used for recording spectra. A Jenway 3345 ion-meter was used for pH measurements.

2.3. Dye removal experiments

Batch-mode adsorption studies were carried out by adding10 mg adsorbent and 10 mL dye solution of known concentration (2.5×10^{-5} mol L^{-1}) in beaker. pH of the solutions were adjusted to the desired value. The mixture solutions were shacked for appropriate adsorption time at 25 °C. After dye adsorption, SiO_2-coated Fe_3O_4magnetic nanoparticles were quickly separated from the sample solution using a magnet. The following equation was applied to calculate the dye removal efficiency in the treatment experiments:

$$R\% = (Ci - Cr)/Ci \times 100 \quad (1)$$

where Ci and Cr are the initial and residual concentrations of the dye in the solution, respectively.

2.4. Synthesis of SiO^2-coated Fe_3O_4 magnetic nanoparticles

The SiO_2-coated Fe_3O_4 magnetic nanoparticles were prepared using sol-gel method. Appropriate amounts of iron nitrate ($Fe(NO_3)_3.9H_2O$), tetra ethoxysilane (TEOS) and oxalic acid ($H_2C_2O_4.2H_2O$) were separately dissolved in ethanol. The three solutions were heated up to 50 °C and stirred for 20 min. The TEOS was added to the iron nitrate followed by oxalic acid addition under strong stirring at 60 °C for 2 h. The precipitate composed of iron oxalate and TEOS was progressively hydrolyzed by the hydration water of iron nitrate and mainly oxalic acid, according to the following scheme:

$$Si(OC_2H_5)_4+4H_2O \rightarrow Si(OH)_4+4C_2H_5OH \quad (2)$$

In the acidic condition (pH≈1), $Si(OH)_4$ is condensed with other materials to a homogeneous gel. Then, the monolithic gel was dried at 110 °C in vacuum for 16 h. Finally, the dried powder was calcined (450 °C for 6 h) to produce solid magnetic composite.

2.5. Sample characterization

2.5.1. X-Ray diffraction (XRD)

The XRD patterns of all the precursor and calcined samples were recorded on a Philips X'Pert (40 kV, 30 mA) X-ray diffractometer, using Kα radiation of Cu as source (λ=1.542 Å) and a nickel filter in the 2θ range of 4°-70°.

2.5.2. N_2-adsorption-desorption measurements

Using BET (Brunauer, Emmett and Teller sorption isotherm) and BJH (Barrett–Joyner–Halenda method) methods, the specific surface area, the total pore volume and the mean pore diameter were measured. For these purposes, N_2 adsorption-desorption isotherm is used at liquid nitrogen temperature (-196 ºC) using a NOVA 2200 instrument (Quantachrome, USA). Prior to the adsorption-desorption measurements, all the samples were degassed at 110 ºC in a N_2 flow for 3 h to remove the moisture and other adsorbates.

2.5.3. Scanning electron microscopy (SEM)

The morphologies of the prepared nanoparticles and their precursors were observed by means of an EM-3200 scanning electron microscope (KYKY Technology Development Ltd.).

3. Results and discussion

3.1.1. Characterization of the SiO_2-coated Fe_3O_4 magnetic nanoparticles

Characterization studies were carried out using XRD and SEM techniques. The XRD pattern of the synthesized magnetic nanoparticles is shown in Fig. 1. The actual identified phases for this sample were Fe_2SiO_4 (cubic). Furthermore, the crystallite sizes of the synthesized sample were calculated from the major diffraction peaks using the Debye–Scherrer equation (Klug and Alexander, 1974):

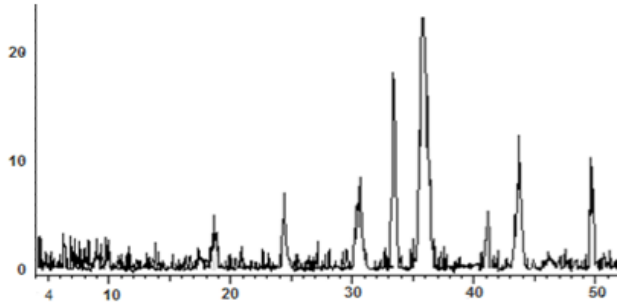

Fig. 1. XRD patterns of the SiO_2-coated Fe_3O_4magneticnanoparticles.

$$D_C = K\lambda/\beta Cos\theta \quad (3)$$

where β is the breadth of the observed diffraction line at its half intensity maximum, K is the so-called shape factor which usually takes a value of about 0.9 and λ is the wavelength of the X-ray source used in the XRD. The crystallite size (Dc) of the SiO_2-coated Fe_3O_4 magnetic nanoparticles was calculated to be 48 nm using the above equation.

The XRD technique may not be sufficiently sensitive to reveal the fine details of these changes. To get this, a detailed SEM study of both precursor and calcined SiO_2-coated Fe_3O_4 magnetic nanoparticles was done and the results are given in Fig. 2. SEM observations show differences in morphology of the precursor and calcined magnetic nanoparticles. The image obtained from the precursor depicts several larger agglomerations of particles (Fig. 2a) and shows that this material has a less dense and homogeneous morphology. After calcination at 450 °C for 6 h and heating rate of 3 °C min^{-1}, the morphological features became different from the precursor sample and the agglomerate size reduced greatly (Fig. 2b). It may be attributed to the covering of calcined magnetic nanoparticle surface by small crystallite of SiO_2, in agreement with XRD results.

Please cite this article as: M. Shariati-Rad, M. Irandoust, S. Amri, M. Feyzi, F. Ja'fari, Removal, preconcentration and determination of methyl red in water samples using silica coated magnetic nanoparticles and central composite design, Journal of Applied Research in Water and Wastewater, 1(1), 2014, 6-12.

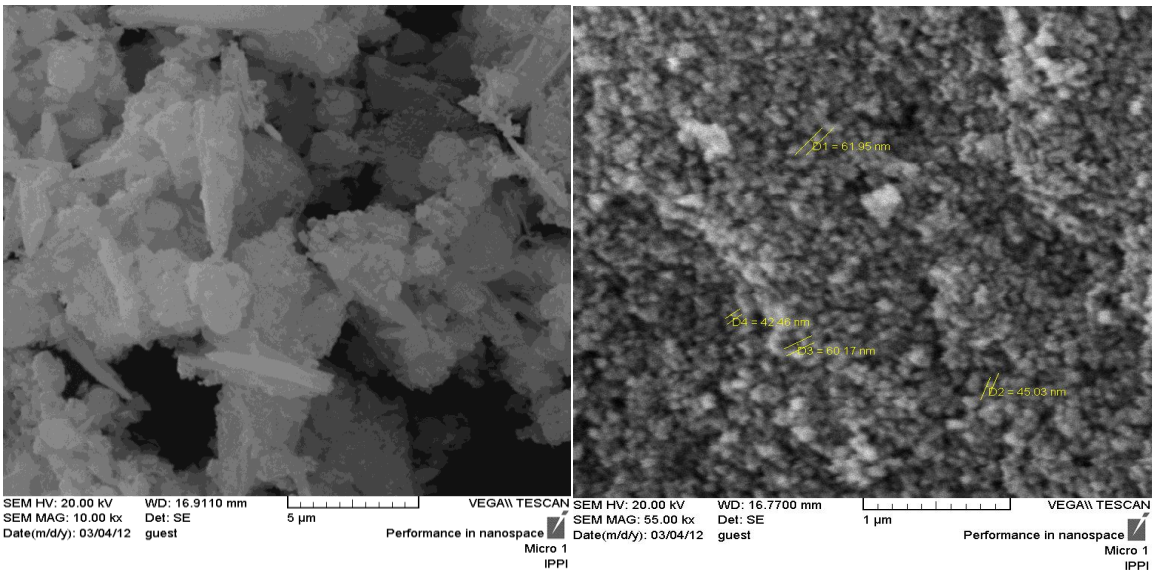

Fig. 2. The SEM image of SiO_2-coated Fe_3O_4 magnetic nanoparticles (a) precursor and (b) calcined sample.

3.1.2. Central composite experimental design for optimization of the parameters

The experimental design technique commonly used for process analysis and modeling is central composite design (CCD) (Gunaraj and Murugan 1999; Box and Hunter 1957). Experimental design methodology involves changing all variables from one experiment to the next, simultaneously. The reason for this is that variables can influence each other and the ideal value for one of them can depend on the values of the others. In this work, we performed CCD. It is assumed that the central point for each factor is 0, and the design is symmetric around this (Brereton 2003).

CCD including the factors, their levels, and the result of each experiment are shown in Table1. Concentration of dye used in these experiments is 2.5×10^{-5} mol L^{-1}.

Table 1. Central composite design and the results of experiments.

Factor		Level		
	1	0	-1	
t(min)	120	70	20	
mg MNPs	10	5.5	1	
pH	5	3	1	
Central composite design				
Run order	*t* (min)	*mg* MNPs	pH	%Removal
1	120	10	1	33.6
2	70	5.5	3	51.2
3	120	10	5	89.27
4	70	10	3	64.64
5	70	5.5	5	73.17
6	20	10	5	82.4
7	20	5.5	3	48
8	70	5.5	3	58.22
9	120	1	5	67.7
10	70	5.5	3	58.4
11	70	1	3	26
12	120	5.5	3	61.6
13	20	1	5	57.6
14	70	5.5	1	9.2
15	70	5.5	3	51.36
16	120	1	1	9.2
17	70	5.5	3	59.52
18	20	1	1	6.8
19	70	5.5	3	58
20	20	10	1	27.2

Analysis of variance for the results of CCD has been given inTable2. As shown in Table 2, pH and the amount of SiO_2-coated Fe_3O_4magnetic nanoparticles (*mg* MNP) are significant factors in the removal of methyl red at 95% confidence level (calculated *p* values for these factors are smaller than 0.05). The pH of the system exerts profound influence on the adsorptive uptake of the dye presumably due to its influence on the surface properties of the adsorbent and ionization/dissociation of the dye. Very low value of the coefficient for *t* in the model indicates that time is not an important factor in the adsorption of methyl red on the SiO_2-coated Fe_3O_4 magnetic nanoparticles. This was experimentally observed.

The solutions of methyl red were rapidly decolored in contact with SiO_2-coated Fe_3O_4 magnetic nanoparticles. Among the squared and interaction terms, pH×pH is statistically important based on the *p* values. The *F* value of the regression is relatively high (with $F = 31.32$ and $p = 0$). This indicates the importance of the regression.

Table 2. Analysis of variance of the experiments in Table 1.

Term	Coefficient	t[a]	p[b]
Constant	-23.478	-2.39	0.038
t	-0.240	-1.07	0.309
*mg*MNP	5.168	2.30	0.045
pH	26.143	4.43	0.001
t ×*t*	0.002	1.40	0.193
*mg*MNP × *mg*MNP	-0.216	-1.20	0.258
pH× pH	-2.128	-2.33	0.042
t × *mg*MNP	0.000	0.04	0.965
t × pH	0.010	0.48	0.644
*mg*MNP × pH	0.022	0.09	0.929
Regression			
R^2 (%)	96.60		
F	31.32		

[a.] Statistical t value.
[b.] Probability value.

Order to gain insight about the effect of each variable, the three dimensional (3D) graphs for the responses were plotted based on the model polynomial function to analyze the variation in the response surface as shown in Fig. 3.These figures show the relationship between two variables and response (Removal%) at center level of the other variables.

It can be seen that in the solutions with weak acidity, the response is higher. This is more evident in Fig. 3c. Moreover, the removal of dye increases with the amount of SiO_2-coated Fe_3O_4 magnetic nanoparticles (*mg*MNP) and *t*.

In the next step, response surface optimization was used to explore the optimum conditions of the factors. Response optimization showed that the Removal% will be maximum at *t* = 120 min, *mg*MNP = 10.0 mg and pH = 5.0.

3.1.3. Mechanism of the interaction

The electrostatic interaction between methyl red and SiO_2-coated Fe_3O_4 magnetic nanoparticles is influenced by solutions pH. Partial ionization of Si-OH could start at low pH values which make the surface of the SiO_2-coated Fe_3O_4 magnetic nanoparticles negatively charged. Methyl red is positively charged at low pH values which favor the electrostatic interaction between SiO_2-coated Fe_3O_4 magnetic nanoparticles and methyl red. Increasing pH causes Si-OH to ionize which provides more electrostatic attraction sites for methyl red.

3.1.4. Study of the kinetics of adsorption

Study of the kinetics of dye adsorption onto SiO_2-coated Fe_3O_4magnetic nanoparticles is required for selection of the optimum operating conditions for the full-scale batch processes. The kinetic parameters which are helpful for the prediction of the adsorption rate give important information for designing and modeling of the adsorption processes (Afkhami and Moosavi 2010). Kinetic studies were performed in a 15 mL glass beaker where 10 mg of SiO_2-coated Fe_3O_4 magnetic nanoparticles was added to 10 mL of the dye solution with different concentrations ranging between 10 mg L^{-1} and 30 mg L^{-1} at room temperature and at pH 5.0. This was followed by shaking by a shaker at 250 rpm to ensure equilibrium is reached. At time *t* = 0 and equilibrium, dye concentrations were measured by UV–Vis spectrophotometry at 521 nm. The amount of adsorption at equilibrium, *qt*(mg/g), was calculated by:

$$qt = (Ci - Ct)V/W \quad (4)$$

where C_i and C_t (in mg L^{-1}) are concentrations of dye in liquid phase at *t* = 0 and equilibrium after time *t* of incubation, respectively. *V* is the volume of the solution (in L) and *W* is the mass of dry SiO_2-coated Fe_3O_4magnetic nanoparticles used (in g).

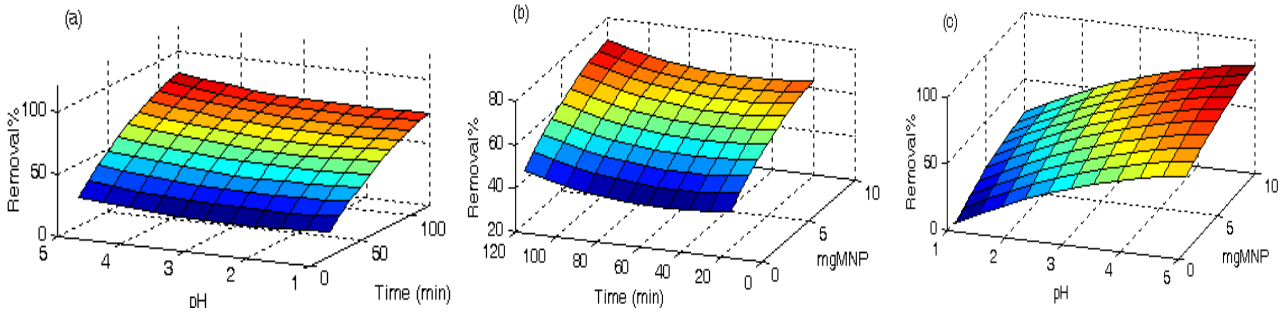

Fig. 3. Variation of response surfaces with pH and *t*
(a), *t* and amount of magnetic nanoparticle (*mg*MNP) and (c) pH and amount of magnetic nanoparticle *(mg*MNP).

The removal rate was very fast during the initial stages of the adsorption process. The kinetic data for adsorption of the dye onto SiO_2-coated Fe_3O_4magnetic nanoparticles were analyzed using pseudo-second order model to find out the adsorption rate expression. The kinetics of adsorption was identified to be a pseudo-second order model. The sorption kinetics for all the initial dye concentrations was treated by Ho's pseudo-second-order rate equation (Chien and Clayton 1980):

$$\frac{t}{qt} = \frac{1}{k_2 qe^2} + \left(\frac{1}{qe}\right) t \quad (5)$$

where *qt* and *qe* are the amounts of adsorbed dye at each time and at equilibrium, respectively. k_2 is the pseudo-second order rate constant. Fitting of the pseudo-second-order kinetic model to the kinetic data is shown in Fig. 4. The pseudo-second-order rate equation constants for all of the initial concentrations used in the experiments are shown in Table 3.

Equilibrium isotherm equations are used to describe the experimental sorption data. The parameters obtained from different models provide important information on the sorption mechanisms, the surface properties and affinities of the sorbent (Shariati et al. 2011). The equilibrium adsorption isotherm model which is the number of *mg* adsorbed of dye per *g* of adsorbent (*qe*) versus the equilibrium concentration of adsorbate is fundamental in describing the interactive behavior between adsorbate and adsorbent (Afkhami et al. 2010). Since, more common models used to investigate the adsorption isotherm are Langmuir and Freundlich equations, these two models were fitted to the experimental data (Qadri et al. 2009).

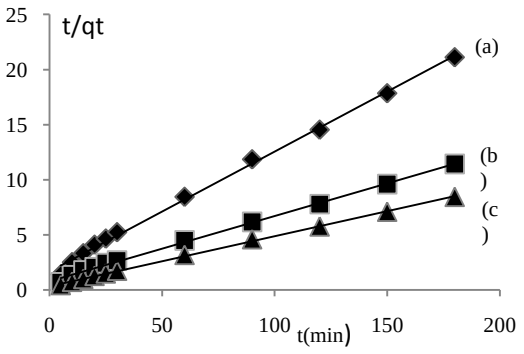

Fig. 4. Kinetics of adsorption based on the pseudo-second-order kinetic model for initial dye concentrations of (a) 10, (b) 20 and (c) 30 mg L^{-1}.

Table 3. Values of the pseudo-second-order rate equation parameters in different initial concentration of dye.

Initial concentration(mg L^{-1})	Equation	*qe* (mg g^{-1})	*k* (g mg^{-1} min^{-1})	R^2
10	*t*/*qt* = 0.1088 *t* + 1.6663	9.19±0.16	0.0072±0.0008	0.9973
20	*t*/*qt* = 0.0591 *t* + 0.7963	16.92±0.24	0.0044±0.0000	0.9982
30	*t*/*qt* = 0.0454 *t* + 0.3364	22.03±0.23	0.0062±0.0007	0.9991

Langmuir's model does not take into account the variation in the adsorption energy, but it is the simplest description of the adsorption process. It is based on the physical hypothesis that the maximum adsorption capacity consists of a monolayer adsorption, there are no interactions between adsorbed molecules and the adsorption energy is distributed homogeneously over the entire coverage surface

(Afkhami and Moosavi 2010). The equilibrium adsorption isotherm was determined using batch studies with different initial concentrations of methyl red (10–100 mg L^{-1}) at 25 °C and at pH 5.0.

The linearized form of the Langmuir isotherm, assuming monolayer adsorption on a homogeneous adsorbent surface, is expressed as (Langmuir 1918):

$$\frac{Ce}{qe} = \frac{1}{K_L q_{max}} + \left(\frac{1}{q_{max}}\right) Ce \quad (6)$$

where q_{max} (in mg g^{-1}) is the maximum amount of the adsorbed dye corresponding to the complete monolayer coverage and illustrates the maximum value of *qe* that can be attained as *Ce* increases. K_L(in L mg^{-1}) is the Langmuir adsorption equilibrium constant related to the energy of adsorption. Values of q_{max} and *b* (K_L/q_{max}) are determined from the linear regression plot of (*Ce*/*qe*) versus *Ce*.

The Freundlich isotherm model is an empirical equation that describes the surface heterogeneity of the sorbent. It considers multilayer adsorption with a heterogeneous energetic distribution of active sites accompanied by interactions between adsorbed molecules (Chatterjee et al. 2009). The linear form of the Freundlich isotherm is:

$$Ln(qe) = LnK_f + \frac{1}{n} Ln\,(Ce) \quad (7)$$

where *Ce* is the equilibrium concentration (in mg L^{-1}), *qe* is the amount adsorbed at equilibrium (mg g^{-1}) and finally, K_f (in (mg g^{-1}) (mg $L^{-1})^n$) and 1/*n* are Freundlich constants depending on the temperature and the given adsorbent–adsorbate couple. *n* is related to the adsorption energy distribution and K_f indicates the adsorption capacity. The values of K_f and 1/*n* can be calculated by the plotting Ln(*qe*) versus Ln(*Ce*). The intercept of the resulted line is Ln (K_f) and 1/*n* is its slope. Value of 1/n indicates that the adsorption intensity of dye onto the adsorbent or surface heterogeneity becomes more heterogeneous as its value gets closer to zero. A value for 1/n below 1 indicates a normal Langmuir isotherm while 1/n above 1 is indicative of the cooperative adsorption (Santhi et al. 2010).

The calculated parameters of the Langmuir and Freundlich isotherms and the correlation coefficients (*r*) are listed in Table 4.Table 4shows that the Langmuir isotherm equation is better fitted to experimental data (*r* is higher relative to *r* for fitting of Frendlich equation to data). It is also evident from these data that the surface of the SiO_2-coated Fe_3O_4magnetic nanoparticles is made up of homogenous adsorption patches than heterogeneous adsorption patches (Faraji et al. 2010). It is generally accepted that under a constant temperature, the *n* values increases with decreasing adsorption energy. This implies that the larger the *n* value, the stronger the adsorption intensity (Belessi et al. 2009). Values of *n*> 1 represent favorable adsorption conditions. In most cases, the exponent between 1<*n*< 10 shows beneficial adsorption (Afkhami and Moosavi 2010).

The essential feature of the Langmuir isotherm can be expressed in terms of a dimensionless constant separation factor (R_L) given by the following equation (Afkhami and Moosavi 2010):

$$R_L = \frac{1}{1+a_L C_0} \quad (8)$$

where a_L parameter is a coefficient related to the energy of the adsorption and increases by increasing the strength of the adsorption bond. The adsorption process can be defined as irreversible (R_L = 0), favorable (0<R_L<1), linear (R_L = 1) or unfavorable (R_L> 1) in terms of R_L (Afkhami et al. 2010). The calculated value of R_L for adsorption of 100 mg L^{-1} solution of methyl red is 0.806. This it is between 0 and 1, thus the adsorption of the dye onto SiO_2-coated Fe_3O_4 magnetic nanoparticles is favorable.

3.2. Analytical studies

3.2.1. Desorption and regeneration

Adsorption of methyl red onto the SiO_2-coated Fe_3O_4magnetic nanoparticles is a reversible process. Therefore, regeneration or activation of the SiO_2-coated Fe_3O_4magnetic nanoparticles to reuse is possible. Desorption of the dye from the SiO_2-coated Fe_3O_4magnetic nanoparticles was studied using different kinds of solvents. Desorption process was performed by mixing 0.01 g methyl red loaded adsorbent with a 2.0 mL volume of EtOH, pure acetic acid, HCl and NaOH solutions with concentrations of 0.1 mol L^{-1}. SiO_2-coated Fe_3O_4magnetic nanoparticles were collected magnetically from the solution. Concentration of dye in the desorbed solution was measured spectrohotometrically. Fig. 5 shows the percentage of the recovered dye. It can be concluded from Fig. 5 that a 2.0 mL volume of 0.1 mol L^{-1}NaOH solution is the most effective eluent for desorption of methyl red from SiO_2-coated Fe_3O_4magnetic nanoparticles. The results showed that desorption efficiencies higher than 99% can be achieved in a short time of 3 min and in a one step elution using 2 mL of 0.1 mol L^{-1} NaOH. Therefore, the dye could be desorbed from the loaded SiO_2-coated Fe_3O_4magnetic nanoparticles by changing the pH of the solution to alkaline range. The SiO_2-coated Fe_3O_4 magnetic nanoparticles were washed with deionized water and reused for two successive removal processes with removal efficiencies higher than 90% (Fig. 6). Under higher removal cycles, removal efficiency decreases. This may be due to oxidation, losing and/or dissolving some amounts of the adsorbent during the successive steps.

Table 4. Parameters of the fitting of experimental data to the Langmuir and Freundlich isotherms equations.

Langmuir isotherm		
a_L (L/mg)	K_L(L/g)	q_{max}|=K_L/ a_L| (mg/g)
R_L	*r*	
0.0024±0.0006	0.12±0.02	49.5±1.76
0.806±0.200	0.9899	
Freundlich isotherm		
K_f	*nr*	
8.33±1.18	2.12±0.22	
0.9221		

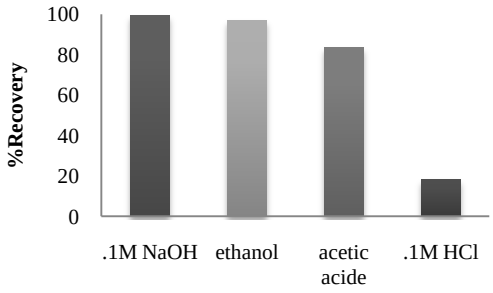

Fig. 5. Percentage of the recovered dye in desorption by different solvents.

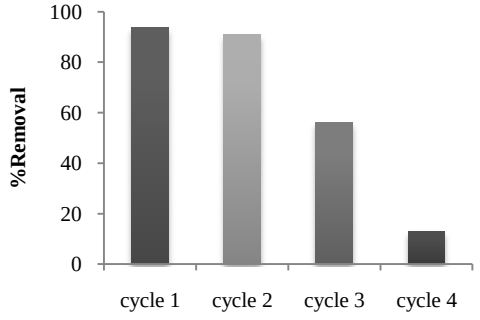

Fig. 6. Removal efficiency for reused SiO_2-coated Fe_3O_4magnetic nanoparticles.

3.2.2. Effect of sample volume

Effect of sample volume on the adsorption of methyl red on 0.01 g of SiO_2-coated Fe_3O_4magnetic nanoparticles was studied in the range of 10-200 mL. In order to study the effect of sample volume, 10 mL of 1 mg L^{-1} solution of methyl red was diluted to 50, 100, 150 and 200 mL with double distilled water. The results showed that the methyl red present in the volumes up to 100.0 mL was completely and quantitatively adsorbed with SiO_2-coated Fe_3O_4 magnetic nanoparticles. At higher volumes percent of recovery decreased.

Therefore, a sample volume of 100.0 mL was selected for determination of trace quantities of methyl red in the samples. This volume is selected in order to increase the preconcentration factor.

3.2.3. Analytical parameters and applications

Increasing concentrations of dye were contacted with SiO_2-coated Fe_3O_4magnetic nanoparticles in optimum adsorption conditions and then, dye was desorpted in optimum conditions. For constructing calibration curve, the spectrophotometric signal of the solution obtained by desorption process was plotted against the initial concentration of dye. Statistical parameters of the calibration curve have been collected in Table 5. As an analytical method, the statistics `of the method in preconcentration and determination of methyl red are very good. As the amount of methyl red in 100.0 mL of the solution was concentrated to 2 mL, a preconcentration factor of 50 was achieved in this method.

The suitability of the proposed method for the analysis of natural water samples was checked by spiking samples of river water with 25, 100, 175 ng mL^{-1} of methyl red. The results have been given in Table 6. The results in Table 6 show the good accuracy (percent recoveries close to 100) and precision (RSD% below 1) of the method.

The maximum adsorption capacity (qmax) for the adsorption of methyl red onto SiO2-coated Fe3O4magnetic nanoparticles calculated from the Langmuir isotherm model is 49.50 mg g−1. In the only reported adsorption study of methyl red based on the activated carbon as adsorbent (Santhi et al. 2010), the obtained value for qmax is 40.486 mg g^{-1}.

Table 5. Statistical results of the preconcentration and calibration of methyl red by the proposed method (Miller and Miller 2005).

Parameter	Characteristic
Number of samples	10
Linear range (ng mL−1)	25.0-250.0
Slope	0.0025
Standard error of slope	1.72×10-4
Intercept	0.0741
Standard error of intercept	0.0266
Correlation coefficient	0.9922
Detection limit(ng mL−1)	0.174

Comparison shows that the adsorbent used in the present work have nearly 25% higher capacity for adsorption of methyl red. Besides that, magnetic and electronic properties that cause simple magnetic separation of methyl red loaded adsorbent makes these particles as good candidate for methyl red adsorption.

Table 6. Results of the analysis of the water samples by the proposed method.

Sample	Amount added (ng mL^{-1})	Amount detected (ng mL^{-1})	RSD%	Recovery%
River water				
	0.0	n.d.[a]	-	-
	25.0	25.74±0.01[b]	0.69	97.12
	100.0	100.56±0.01[b]	0.60	99.44
	175.0	175.62±0.02[b]	0.48	99.64

[a.] Not detected.
[b.] Standard deviations were calculated based on three determinations.

4. Conclusion

Silica coated magnetic nanoparticles were synthesized and utilized for preconcentration, determination and removal of methyl red in aqueous solutions. UV–Vis absorption spectrophotometry was used to study the adsorption behavior of methyl red after treatment by the adsorbent. For adsorption of methyl red in water samples, the prepared magnetic nanoparticles can be easily dispersed and then separated by a magnet. The proposed method is novel, safe, convenient, rapid and inexpensive for preconcentration, determination and infiltration of methyl red as a toxic compound from waste water. The maximum efficiency of the adsorbent was observed in mild conditions with pH 5.0. The pseudo-second-order kinetic model fitted well with the kinetics of the dye removal. The Langmuir model was fitted better to the dye removal data relative to the Freundlich model. The magnetic particles can be washed and recycled for two dye adsorption cycles.

Reference

Afkhami A., Saber-Tehrani M., Bagheri H., Modified maghemite nanoparticles as an efficient adsorbent for removing some cationic dyes from aqueous solution, Desalination 263 (2010) 240-248.

Albornoz C., Jacobo S.E., Preparation of a biocompatible magnetic film from an aqueous ferrofluid, Journal of Magnetism and Magnetic Materials 305 (2006) 12–15.

Aleboyeh A., Aleboyeh H., Effects of gap size and UV dosage on decolorization of C. I. Acid Orange 7 by UV/H_2O_2 process, Journal of Hazardous Materials 133 (2006) 167–171.

Belessi V., Romanos G., Boukos N., Lambropoulou D., Trapalis C., Removal of Reactive Red 195 from aqueous solutions by adsorption on the surface of TiO_2 nanoparticles, Journal of Hazardous Materials 170(2009) 836–844.

Box G.E.P., Hunter J.S., Multi-factor experimental designs for exploring response surfaces, Ann. Math. Stat 28 (1957) 195-241.

Bucak S., Jones D.A., Laibinis P.E., Hatton T.A., Protein separations using colloidal magnetic nanoparticles, Biotechnology Programe 19 (2003) 477-484.

Bulte J.W.M., Intracellular endosomal magnetic labeling of cells, Methods Mol. Med 124 (2006) 419–439.

Chien S.H., Clayton W.R., Application of Elovich equation to the kinetics of phosphate release and sorption on soils, Soil Science society American Journal 44 (1980) 265–268.

De Sales P.F., Magriotis Z.M., Rossi M.A.L.S., Resende R.F., Nunes C.A., Optimization by Response Surface Methodology of the adsorption of Coomassie Blue dye on natural and acid-treated clays, Journal of Environmental Management 130 (2013) 417-428.

Faraji M., Yamini Y., Tahmasebi E., Saleh A., Nourmohammadian F., Cetyltrimethylammonium bromide-coated magnetite nanoparticles as highly efficient adsorbent for rapid removal of reactive dyes from the textile companies' wastewaters, Journal of Iranian Chemical Society 7 (2010) 130–144.

Gómez V., Callao M.P., Modeling the adsorption of dyes onto activated carbon by using experimental designs, Talanta 77 (2008) 84-89.

Juang R.S., Wu F.C., Tseng R.L., Characterization and use of activated carbons prepared from bagasse for liquid-phase adsorption, Colloids Surface: A 201 (2002) 191–199.

Klug H.P., Alexander L.E., X-ray Diffraction Procedures for Polycrystalline and Amorphous Materials, second ed., Wiley, New York, 1974.

Please cite this article as: M. Shariati-Rad, M. Irandoust, S. Amri, M. Feyzi, F. Ja'fari, Removal, preconcentration and determination of methyl red in water samples using silica coated magnetic nanoparticles and central composite design, Journal of Applied Research in Water and Wastewater, 1(1), 2014, 6-12.

Langmuir I., The adsorption of gases on plane surfaces of glass, mica and platinum, Journal of American Chemical Society 40 (1918) 1361–1403.

Laurent S., Forge D., Port M., Roch A., Robic C., Vander Elst L., Muller R.N., Magnetic iron oxide nanoparticles: synthesis, stabilization, vectorization physicochemical characterizations, and biological applications, Chemical Review 108 (2008) 2064–2110.

Miller J.N., Miller J.C. (Eds.), Statistics and Chemometrics for Analytical Chemistry, fifth ed., Pearson Education Limited, London, 2005, p. 114.

Mirsha A., Bajpaj M., The flocculation performances of Tamarindus Mucilage in relation to removal of vat and direct dyes, Bioresource Technology 97 (2006) 1055–1059.

Qadri S., Ganoe A., Haik Y., Removal and recovery of acridine orange from solutions by use of magnetic nanoparticle, Journal Hazardous Materials 169 (2009) 318-323.

Ravikumar K., Ramalingam S., Krishnan S., Balu K., Application of response surface methodology to optimize the process variables for Reactive Red and Acid Brown dye removal using a novel adsorbent, Dyes Pigments 70 (2006) 18-26.

Sahoo C., Gupta A.K., Optimization of photocatalytic degradation of methyl blue using silver ion doped titanium dioxide by combination of experimental design and response surface approach, Journal Hazardous Materials 215 (2012) 302-310.

Santhi T., Manonmani S., Smith T., Removal of methyl red from aqueous solution by activated carbon prepared from the anonna a squmosa seed by adsorption, Chemical Engineering Research Bulletin 14 (2010) 11-18.

Shariati S., Faraji M., Yamini Y., Rajabi A.A., Fe_3O_4 magnetic nanoparticles modified with sodium dodecyl sulfate for removal of safranin O dye from aqueous solutions, Desalination 270 (2011) 160-165.

Singh K.P., Gupta S., Singh A.K., Sinha S., Optimizing adsorption of crystal violet dye from water by magnetic nanocomposite using response surface modeling approach, Journal Hazardous Materials 186 (2011) 1462-1473.

Sun G., Xu X., Sunflower stalks as adsorbents for color removal from textile wastewater, Industrial Engineering Chemical Research 36 (1997) 808–881.

Torrades F., García-Montaño J., Using central composite experimental design to optimize the degradation of real dye wastewater by Fenton and photo-Fenton reactions, Dyes Pigments 100 (2014) 184-189.

Tuutijarvi T., Lu J., Sillanp M., Chen G., As(V) adsorption on maghemite nanoparticles, Journal Hazardous Materials 166 (2009) 1415–1420.

White B.R., Stackhouse B.T., Holcombe J.A., Magnetic-Fe_2O_3 nanoparticles coated with poly-l-cysteine for chelation of As(III), Cu(II), Cd(II), Ni(II), Pb(II) and Zn(II), Journal Hazardous Materials 161 (2009) 848–850.

Xie X., Zhang X., Yu B., Gao H., Zhang H., Fei W. Rapid extraction of genomic DNA from saliva for HLA typing on microarray based on magnetic nanobeads, Journal of Magnetism and Magnetic Materials 280 (2004) 164–168.

Zhou L., Wang Y., Liu Z., Huang Q., Characteristics of equilibrium, kinetics studies for adsorption of Hg(II), Cu(II), and Ni(II) ions by thiourea modified magnetic chitosan microspheres, Journal Hazardous Materials 161 (2009) 995–1002.

Zuorro A., Fidaleo M., Lavecchia R., Response surface methodology (RSM) analysis of photodegradation of sulfonateddiazo dye Reactive Green 19 by UV/H2O2 process, Journal of Environmental Management 127 (2013) 28-35.

Please cite this article as: M. Shariati-Rad, M. Irandoust, S. Amri, M. Feyzi, F. Ja'fari, Removal, preconcentration and determination of methyl red in water samples using silica coated magnetic nanoparticles and central composite design, Journal of Applied Research in Water and Wastewater, 1(1), 2014, 6-12.